Maritime Technology and Research

https://so04.tci-thaijo.org/index.php/MTR

Research Article

Numerical simulation on hydrodynamic performance of parallel twin vertical axis tidal current turbines

Ke Sun*, Zhou Xuehan, Li Yan and Zhang Liang

College of Shipbuilding Engineering, Harbin Engineering University, Harbin 150001, China

Article information

Received: March 6, 2019
Revised: April 19, 2019
Accepted: April 30, 2019

Keywords

Tidal current energy,
Vertical-axis hydro-turbine,
Hydrodynamic performance,
Parallel twin turbines,
Wake flow

Abstract

Single and parallel twin vertical axis hydro turbines were numerically simulated by using OpenFOAM software, studying the interference effects, such as torque and load of turbine, as well as hydrodynamic performance influenced by the distance and rotation forms between twin turbines, and analyzing the wake flow field to show the velocity profile distribution. The results showed that the average power of parallel twin turbines is always higher than the power of a single turbine, and the closer the lateral distance between turbines, the higher the power. When lateral distance approximates to 1.25 times turbine diameter, and turbines rotate in the opposite inward direction, the average energy efficiency value of parallel twin turbines is about 25 % higher than that of a single one. Additionally, opposite inward rotation is the best arrangement form for twin turbines to obtain more power and counteract lateral force.

1. Introduction

As a marine renewable energy, tidal current energy is a kinetic energy generated by regular flow caused by steady flow and tide in a benthonic channel and strait. Compared with other kinds of ocean energy resource, tidal current energy has a higher energy density, a steady period, a steady load, and abundant reserves. It is estimated that the total theoretical reserves of tidal current energy around the world is about 10^8 kW (Zhang et al., 2013; Dai et al., 2010). Therefore, the large-scale development and utilization of tidal current energy can relieve energy supply and environmental pollution problems in local areas.

The hydro-turbine is one of the main energy capture devices for tidal current energy. At present, in large-scale tidal power stations, the power generation capacity of traditional single turbine systems is very limited; however, large-scale turbine arrays can improve the economic benefits of power stations (Gebreslassie et al., 2012). Multi-unit tidal power stations can not only obtain more energy in limited tidal current fields, but also greatly reduce the cost of single turbines, owing to mass-produced manufacture. Moreover, it is more convenient to maintain and operate power stations. Therefore, multi-unit turbine array tidal power station research has great advantages and the prospect of development.

Many researchers have studied vertical axis tidal turbine arrays. Li and Calisal (2010a; 2011) studied twin turbine arrays by the discrete vortex method and found that the decisive factor of turbine

*Corresponding author: College of Shipbuilding Engineering, Harbin Engineering University, Harbin 150001, China
E-mail address: sunke@hrbeu.edu.cn

energy efficiency was flow direction distance between parallel vertical axis turbine arrays. Goude and Agren (2010) studied the energy efficiency of 5 groups of vertical axis turbine arrays by using the 2-dimensional vortex method, after comparing and analyzing the advantages and disadvantages of a parallel arrangement scheme, as well as a staggered arrangement scheme; the total output power of staggered arrangement turbine arrays was higher than that of parallel arrangement schemes. Although the vortex method takes much less time to operate than the Reynolds-Average Navier Stokes method (RANS), the computational accuracy of vortex method is less accurate than RANS. Dyachuk et al. (2012) studied single-row parallel turbines and analyzed the influence of the distance between 10 parallel turbines and the inlet angle on the output power of each turbine; the results showed that the output power of turbines was sensitive to the inlet angle variation. Guo (2013) systematically studied multi-unit vertical axis tidal turbine array arrangement by the CFD method; the research revealed that smaller lateral distance of parallel turbine array can efficiently improve turbine power coefficient, and the rotation direction of a turbine had little effect on the turbine's total output power. However, Guo (2013) did not study the hydrodynamic performance of parallel twin turbines, which is very different from the parallel 3 turbines in his research. Wang and Sun (2016) numerically simulated parallel twin-turbines by the transient CFD method, researching the influence of the initial position angle between 2 groups of 2 blade turbines on turbine hydrodynamic performance; the results showed that the total output power of twin turbines was more than twice the output power of single turbines, especially at medium high speed ratio working conditions. Lee and Hyun (2016) studied the influence of the rotation direction, as well as the distance between turbines on the output power of turbine sets; the research results showed that the output power of twin turbines of opposite inward rotation direction was higher, and the energy efficiency was about 9.2 % higher than that of a single turbine. However, Lee and Hyan (2016) did not analyze the torque and load of the parallel twin turbines, which is crucial to turbine design. Patel et al. (2017) carried out a series of experimental investigations of Darrieus straight blade turbines, studying the hydrodynamic performance of difference in streamwise distance, as well as lateral distance, of twin turbines; the research revealed that a minimum distance of 3D along the spanwise direction is essential in a hydro farm using Darrieus turbines. However, the solidity of the turbines (0.341) in the experiment was too large, which is quite different from practical application. Yong et al. (2018) studied twin rotor turbines from 3 aspects, including blade forces, power output efficiency, and wake flow field; the results indicated that the power output of the twin rotors reaches peak value when the ratio between the 2 main axis distance and diameter of the turbine is around 9/4. However, the total load of the twin turbine system, as well as the hydrodynamic performance influence of rotation direction, are ignored in this research.

In this paper, single and parallel twin vertical axis hydro turbines were numerical simulated by using OpenFOAM software, studying the influence of the distance between turbines and rotation forms on turbine array interference effect, as well as hydrodynamic performance characteristics, in order to optimize the layout scheme of twin vertical axis tidal turbines.

2. Numerical simulation

In this article, an H-type straight blade vertical axis hydro turbine with NACA aerofoil is selected as the research model. Due to it having the same shape of the cross-section of wing span direction, compared with the 3-dimensional simulation method, 2-dimensional simulation will not only save calculation time by greatly reducing grid numbers, but also keep an accepted calculation accuracy. Hence, the 2-dimensional simulation method is adopted for numerical simulation based on the following simplification: (a) Neglect the 3-dimensional effect of blades; (b) Neglect the influence of free surface and water bed; (c) Neglect the influence of main shaft, spoke, and other additional structures; (d) Assume the incoming flow is a uniform flow. The geometry of the physical model is listed in **Table 1**.

Table 1 Geometric parameters of the turbine model.

Parameter	Symbol	Value
Hydrofoil	-	NACA0022
Number of blades	Z	3
Turbine diameter	D	6 m
Chord length	C	0.7 m
Blade deflection	φ	–3°
Incoming flow velocity	V_A	3 m/s

2.1 Coordinate and parameter definition

The Cartesian coordinate system of single vertical axis hydro-turbines is shown in **Figure 1**. The origin of the global coordinate system is located at the center of turbine, the X axis direction is the same as the direction of the incoming flow, and the Y axis direction passes the origin and is perpendicular to the direction of the incoming flow. θ is the position angle of blade, in which anticlockwise rotation is positive, while taking positive X axis as the starting point. The origin of the local coordinate system is at the center of every blade, and the X axis direction and Y axis direction are the same as the direction of the global X and Y direction. The deflection angle φ is defined by the angle between the chord length direction of blade and the tangential direction of the blade's circular locus, and the angle φ of the fixed angle vertical axis hydro-turbine remains –3° in this model.

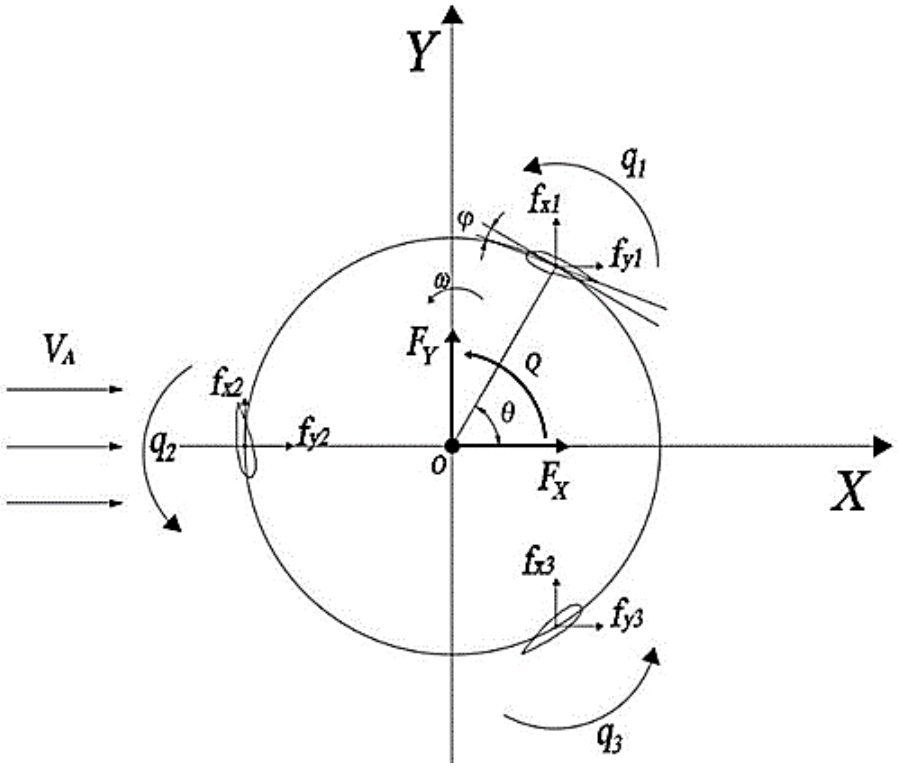

Figure 1 Vertical axis hydro turbine coordinate system.

In order to analyze the calculating data conveniently, the main dimensionless parameters are defined as follows;

$$\lambda = \frac{\omega R}{V_A} \tag{1}$$

$$C_{F_X} = \frac{F_X}{0.5\rho {V_A}^2 DH} \tag{2}$$

$$C_{F_Y} = \frac{F_Y}{0.5\rho {V_A}^2 DH} \tag{3}$$

$$C_q = \frac{q}{0.5\rho {V_A}^2 DHR} \tag{4}$$

$$C_P = \frac{Q\omega}{0.5\rho {V_A}^3 DH} \tag{5}$$

$$\eta = \frac{Cp1+Cp2}{2} \tag{6}$$

where λ, C_{F_X}, C_{F_Y}, C_q, C_P, and η are the tip speed ratio (TSR), thrust coefficient, lateral force coefficient, blade torque coefficient, power coefficient of the single turbine, and average energy efficiency of the twin turbines, respectively. R(m) is turbine radius, which is half of the turbine diameter D; ω(rad/s) is turbine angular velocity; V_A(m/s) is uniform incoming velocity; H(m) is wing span, which is unit length in 2D model; ρ(kg/m^3) is fluid density, which is 1,025 for sea water; q(N·m) is the torque of a single blade on the main shaft; Q(N·m) is the total torque of turbine, $Q = \sum_{i=1}^{3} q_i$;F_X(N) is the overall thrust of turbine, $F_X = \sum_{i=1}^{3} f_x$; F_Y(N) is the overall lateral force of turbine, $F_Y = \sum_{i=1}^{3} f_y$; η is the average energy efficiency of turbine1 and turbine2 in **Figure 2**.

2.2 Computational domain

The twin turbines are placed parallel from a lateral direction, and the absolute value of the turbine axis relative position angle Ψ is 90°. **Figure 2** shows the computational domain of the parallel turbine and the boundary condition. The lateral distances D_y are set at 1.25D, 1.5D, 1.75D, 2.0D, 3.0D, and 4.0D, respectively.

In studying the influence of the rotation direction on the hydrodynamic performance of parallel turbines, CFD numerical simulation of 3 kinds of parallel turbine rotation forms are carried out, which are: same rotation, opposite inward rotation and opposite outward rotation, as shown in **Figure 3**.

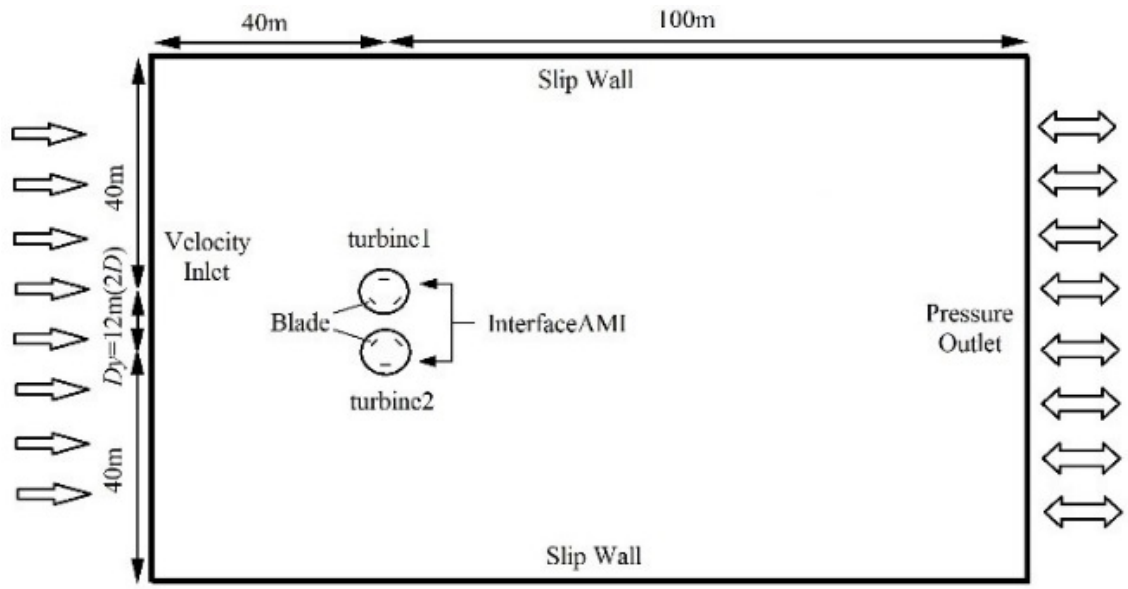

Figure 2 Computational domain of parallel turbines.

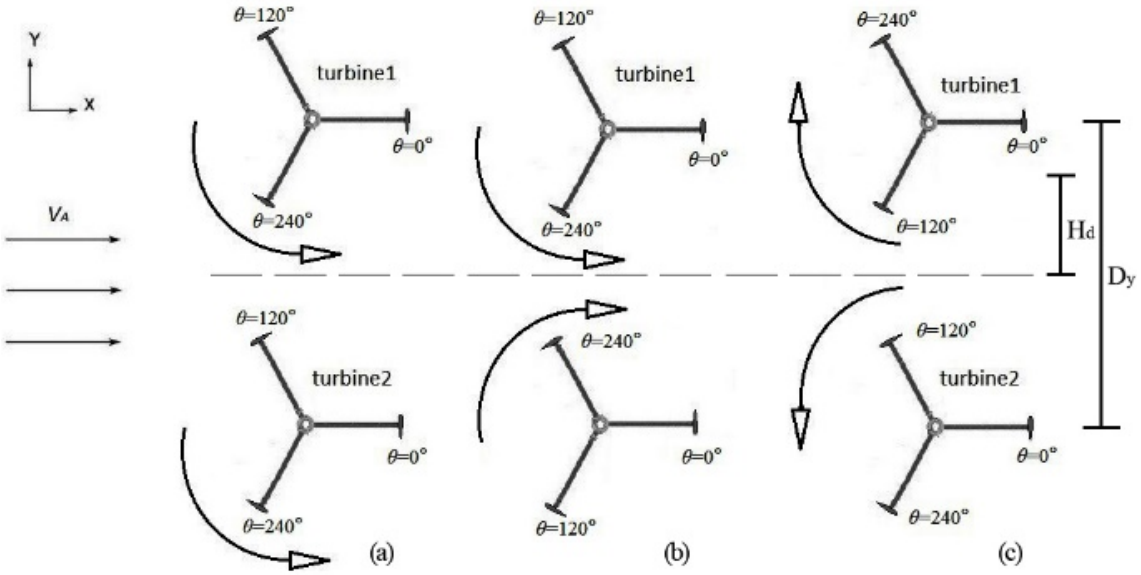

Figure 3 Rotation form illustration of twin turbines; (a) Same rotation; (b) Opposite inward rotation; (c) Opposite outward rotation.

3. Single turbine model validation

A grid of the single turbine model is shown in **Figure 4**. The whole calculation model is divided into 2 parts: rectangular outer flow field, and circular rotating field containing blades. The single turbine model size and parameters of flow field are the same as the parallel turbine model.

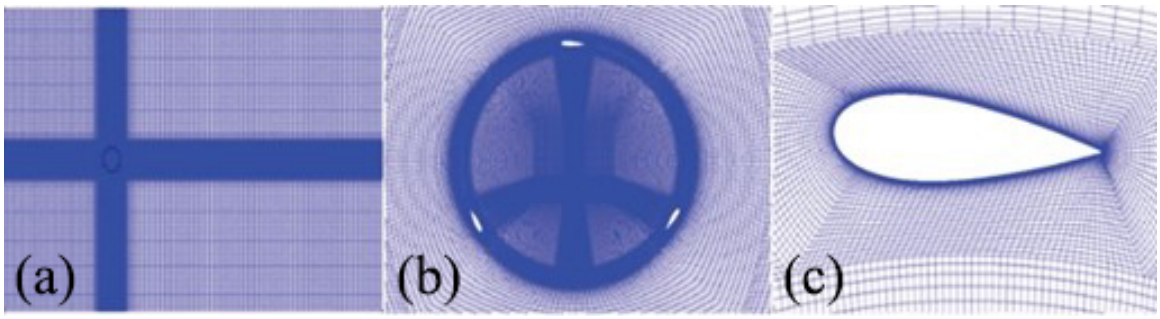

Figure 4 Grid of the single turbine model; (a) Grid in outer domain; (b) Grid in rotating domain; (c) Grid near the blade.

The parameters of the OpenFOAM calculation for the single turbine model, as well as the parallel turbine model, are selected, including grid, time step, turbulence model, turbulence intensity of velocity inlet, and so on (Sun et al., 2017). **Table 2** lists the parameters of CFD analysis.

Table 2 Parameters of CFD analysis.

Parameter	Value
Total grid number	121,000
Rotation domain grid number	85,000
y^+	5
Time step	0.001 s
Solver	PimpleDyMFoam
Turbulence model	*k-ω* SST
Computer configurations	Intel Core i5-4570 3.20 GHz, 8 GB RAM
Computation time of medium mesh quality numerical model	12 h

3.1 Mesh sensitivity analysis

Computational accuracy and simulated time are closely related with the mesh quality of a numerical model. Although finer mesh can better describe physical characteristics, simulated time will increase greatly; therefore, both simulated time and computational accuracy should be considered at the same time when generating mesh. In this paper, 3 different grid quality models are compared and analyzed; detailed information on the grid models are shown in **Table 3**.

Table 3 Mesh sensitivity analysis.

Mesh quality	Total no. of elements	No. of rotation domain elements	y^+
Rough	45,000	25,000	48
Medium	119,000	69,000	6
Fine	274,000	201,000	2

The dimensionless wall distance (y^+) is a dimensionless coefficient which can represent the first-row thickness in numerical simulation. Generally, the first-row thickness in an appropriate value range can ensure the simulated value is similar to the true value.

Figure 5 shows the single blade torque coefficient curve of 3 different mesh models. The torque coefficient of the rough mesh model is quite different from the other models when the azimuthal angle is between 150 and 210°, and the torque coefficient of the medium mesh model, as well as the fine mesh model, have a minor difference, and almost coincide. Owing to the medium mesh model being basically grid independent, and the simulated time of the medium mesh model being shorter than the fine mesh model, the medium mesh model is selected as the calculating model, in order to save simulation time.

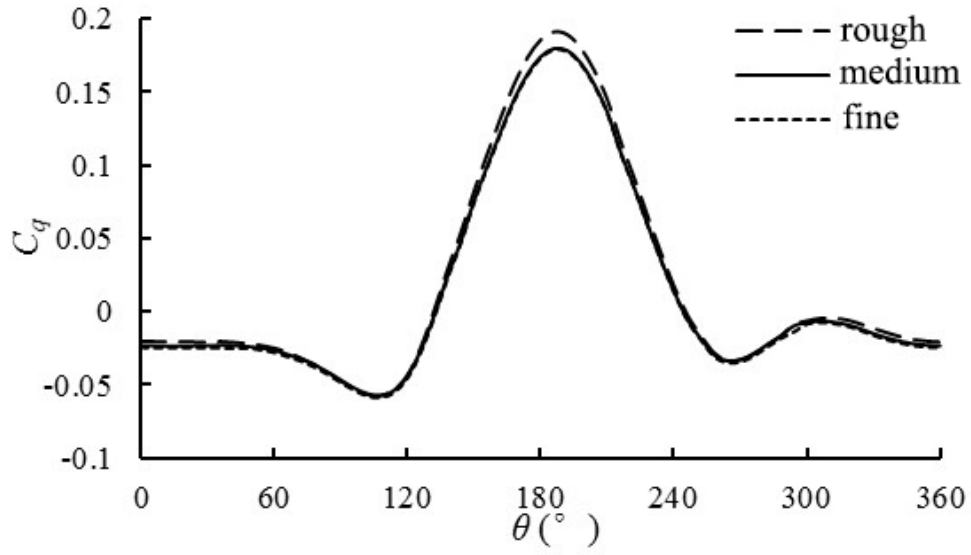

Figure 5 Single blade torque coefficient (mesh sensitivity analysis).

3.2 Experimental validation

For validating the availability of the 2-dimensional numerical model based on Open-FOAM code, a single vertical axis hydro turbine, tested by Peter Bachant, is selected as a verifiable example. **Figure 6** shows the comparison curves of the calculated value and experimental value of the turbine average power coefficient $\overline{C_P}$. 2D calculating value is from the 2-dimensional numerical model by OpenFOAM. The Bachant experimental value comes from test data in reference (Bachant & Wosnik, 2013). Considering the 3-dimensional effect, including tip of blade and support structures, we corrected the 2D calculation data, referring to some conclusions by Li and Calisal (2010b). Blade tip effect will decrease average power coefficient by about 8 %, and support structure will reduce average power coefficient by about 9 % when the turbine wing spandiameter ratio is 1.0. The 3D correction value is corrected by the 2D calculating result, according to the reduction above. It can be seen from the graph that the changing trend of the simulated value has a good agreement with that of the experimental value, both of them reaching the maximum $\overline{C_P}$ at TSR 2.0. The maximum absolute error between the 3D correction value and experimental value of the power coefficient is 4.16 %, which proves that the accuracy of the numerical model for the vertical axis hydro-turbine is acceptable for this article.

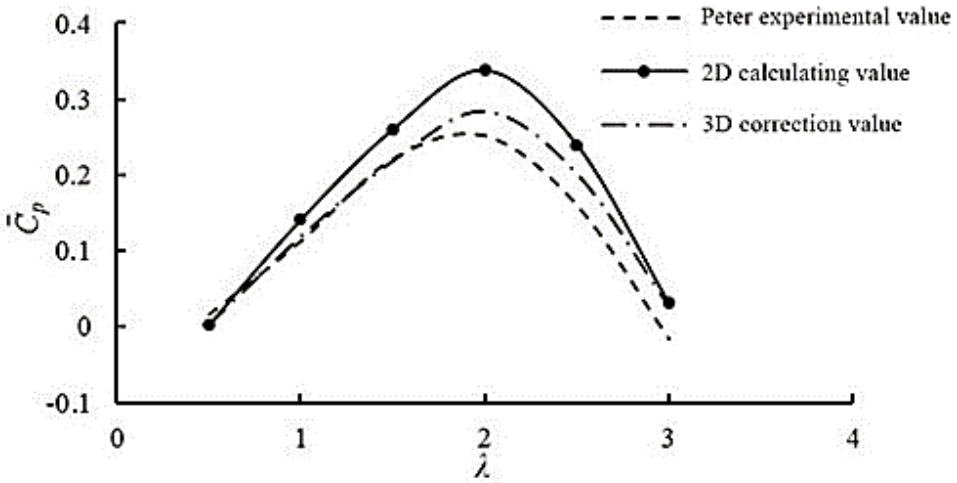

Figure 6 Average power coefficient comparison.

4. Results and discussions

4.1 Single turbine

The most important parameters which measure the hydrodynamic performance of the vertical axis hydro-turbine are average power coefficient $\overline{C_P}$ and blade torque coefficient C_q.

The average power coefficient at different speed ratios of a single turbine can be seen in **Figure 7**. It is shown that turbine power coefficient is highest at TSR 2.0. Therefore, we assume the following 2 parallel turbines rotate at the same angular speed and both TSR at 2.0.

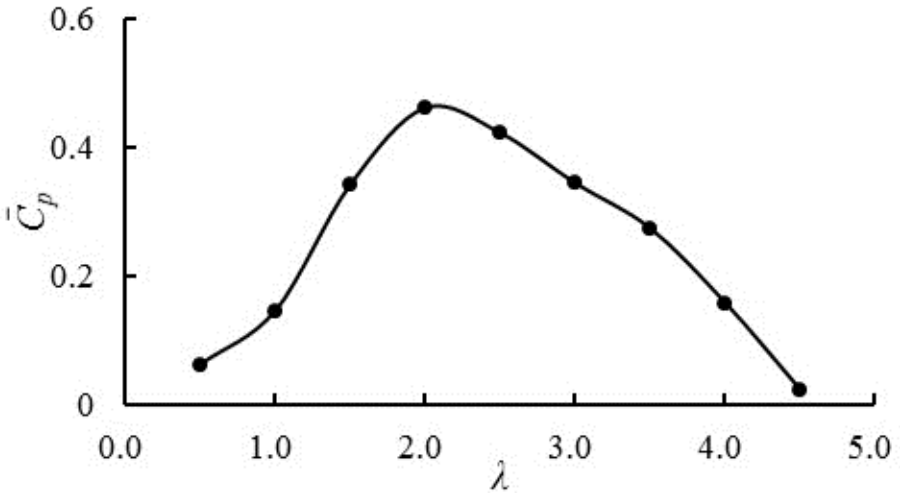

Figure 7 Average power coefficient of the single turbine.

Figure 8 shows the changing curve of single blade torque coefficient C_q with different blade position angles when TSR is 1.0, 2.0, 3.0, and 4.0. It is shown that blade torque is higher when blade position angle ranges from 120° to 240°, and the torque peak is around 180°. Therefore, the main area which provides torque is at the upstream disk of the turbine.

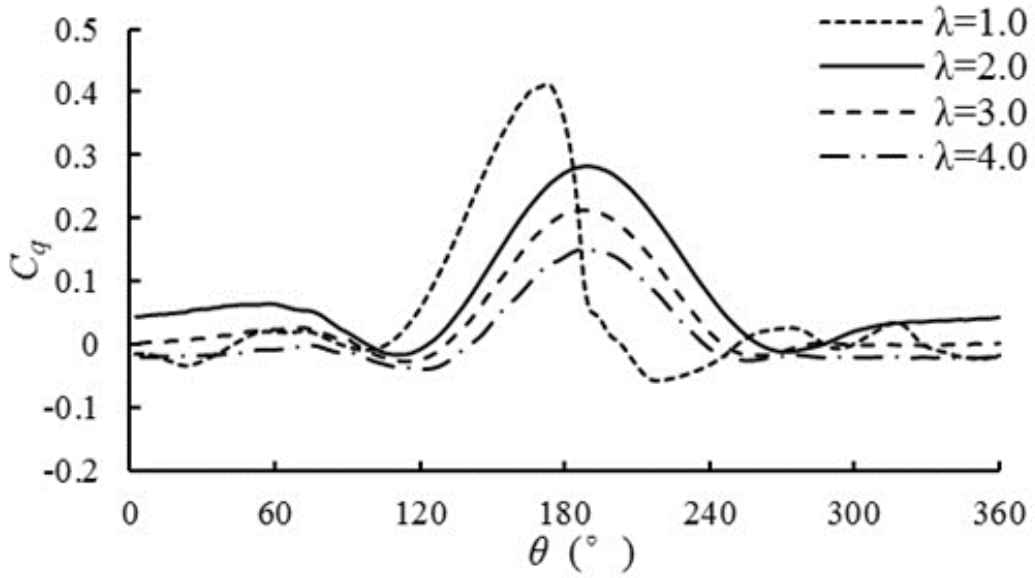

Figure 8 Single blade torque coefficient.

4.2 Parallel turbine

Lateral distance D_y and different rotating forms of parallel turbines are studied for exploring the turbine hydrodynamic performance.

4.2.1 Average energy efficiency

Figure 9 shows average energy efficiency changing curves of parallel turbines in 3 rotating forms with different lateral distance D_y. When the lateral distance between turbines is from 1.25D to 4.0D, average energy efficiency η of the twin turbines is higher than that of the single turbine at any rotating form caused by the blockage effect of turbines. The highest is the opposite inward rotation direction, the second highest is the same rotation direction, and the lowest is the opposite outward rotation direction. The average energy efficiency decreases with increase of lateral distance. Therefore, theoretically, the smaller the distance, the more power output. However, too small lateral distance between turbines will make difficulty in the installation and daily maintenance of equipment.

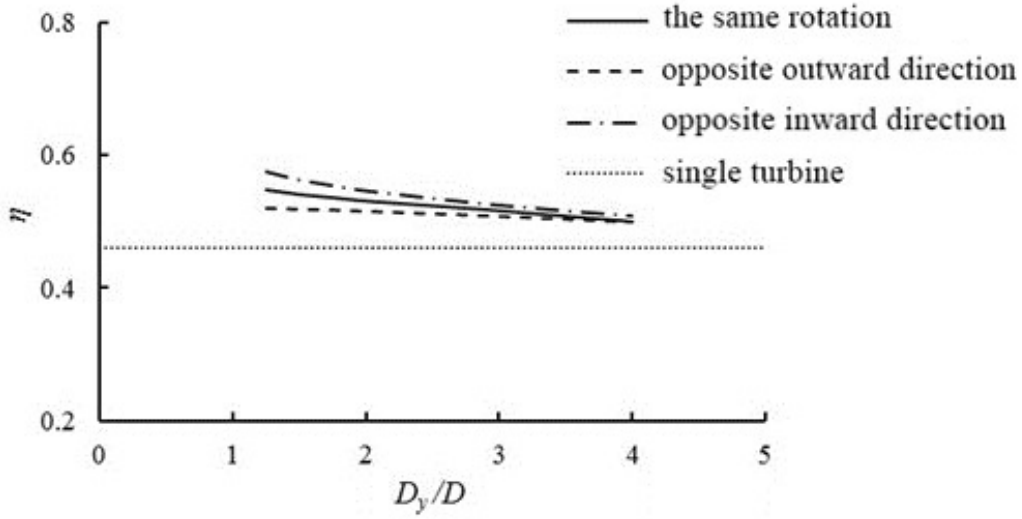

Figure 9 Average energy efficiency comparison at 3 rotating forms with different lateral distance.

4.2.2 Blade torque coefficient

In studying blade mechanical characterristics in the running process of parallel turbine, 3 lateral distances of turbine are set D_y=1.5D, 2.0D, and 4.0D. Here, T1 and T2 represent the blade torque on turbine1 and turbine2.

Figures 10 - 12 are individual blade torque coefficients of each turbine with 3 rotation forms at 3 lateral distances, in which it can be seen that each blade torque of the parallel turbine is clearly higher than the single turbine blade when the position angle range is from 120 to 270°. If the lateral distance is smaller, the average value and the maximum value of blade torque coefficient is higher. With increasing lateral distance, the blade torque coefficient gradually become smaller and closer to that of the single turbine.

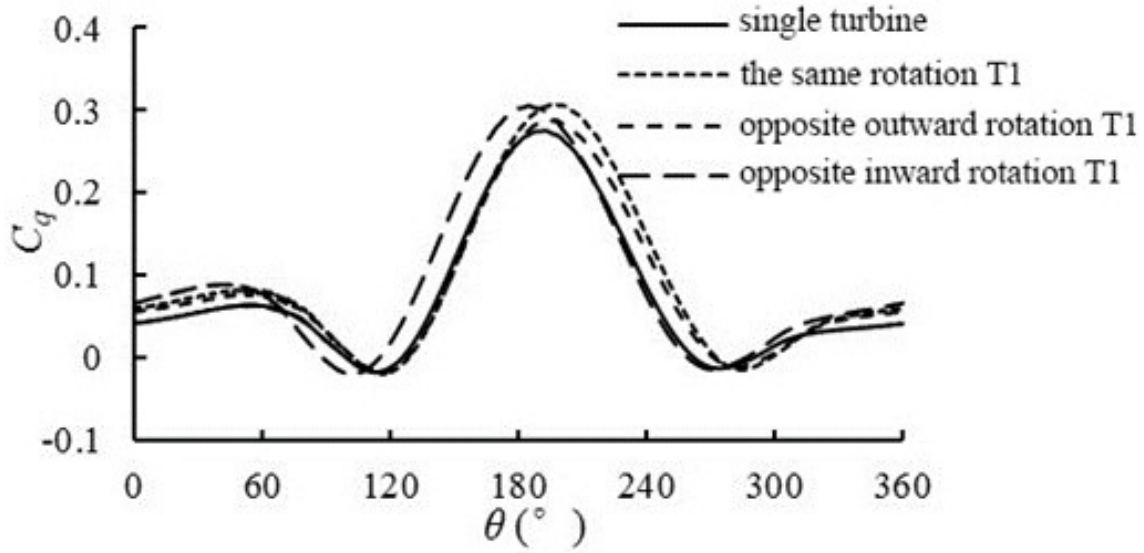

(a) Turbine1-blade

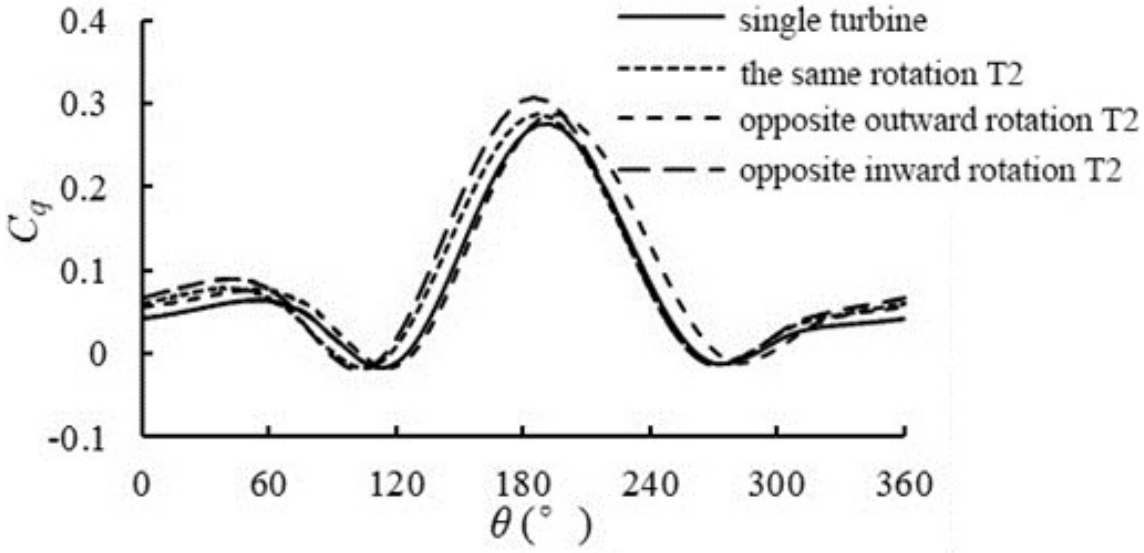

(b) Turbine2-blade

Figure 10 Blade torque coefficient with different rotation forms (D_y = 1.5D).

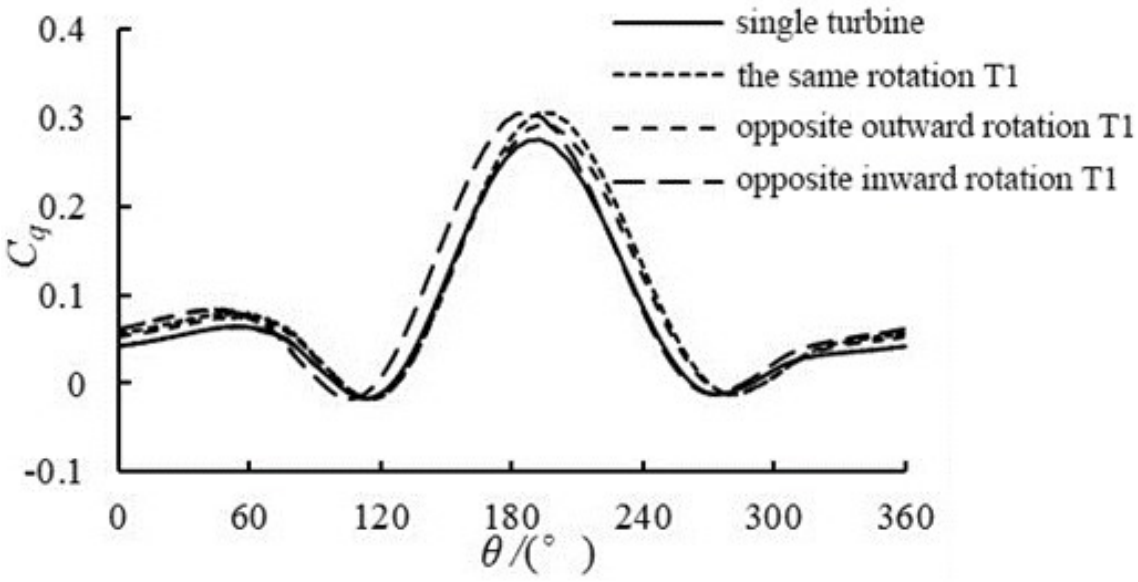

(a) Turbine1-blade

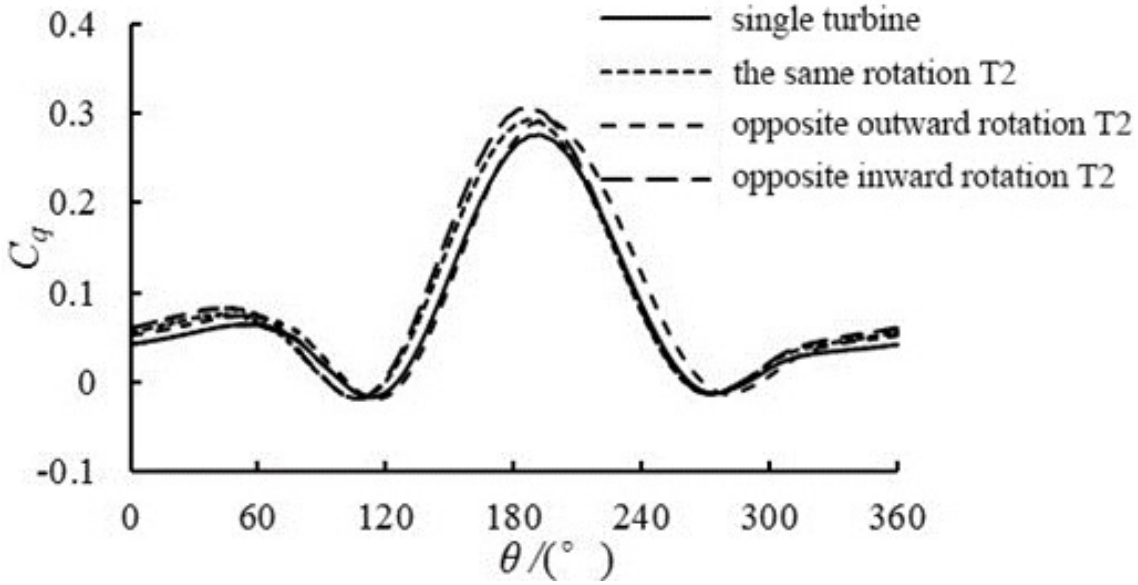

(b) Turbine2-blade

Figure 11 Blade torque coefficient with different rotation forms (D_y = 2.0D).

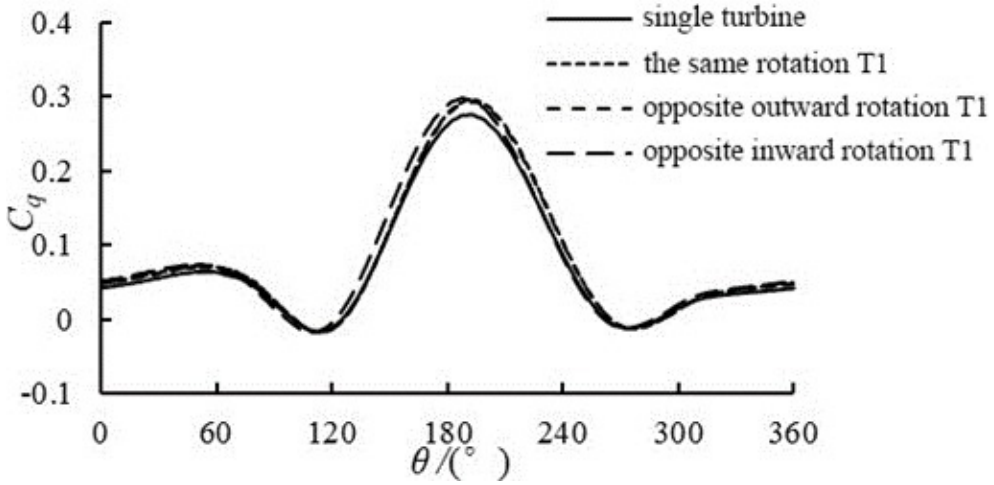

(a) Turbine1-blade

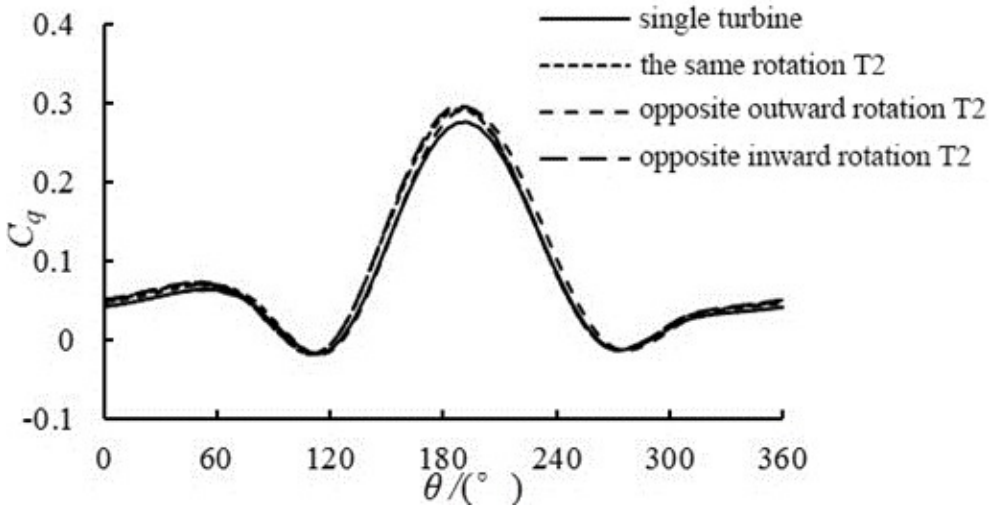

(b) Turbine2-blade

Figure 12 Blade torque coefficient with different rotation forms (D_y = 4.0D).

In addition, for rotating in the same direction, the average blade torque coefficient of turbine1 is higher than that of turbine2, and the position angle of turbine1 when blade torque reaches the maximum is earlier than turbine2. This difference is caused by the asymmetry of flow field. For opposite inward rotation and opposite outward rotation, 2 turbines have nearly the same blade torque, owing to its symmetric layout. The turbine's power derives from the torque of each blade. Therefore, the output power of 2 turbines are entirely the same at 2 opposite rotation forms.

4.2.3 Thrust and Lateral force of Turbine

Because twin turbines are usually installed on one carrier platform, the thrust and lateral force of turbines are of vital importance for loads directly applied on the carrier platform. To study the influence of twin turbine rotation forms, we keep one fixed lateral distance D_y = 1.5D. Thrust and lateral force of parallel turbines in one rotating period are shown in **Figures 13** and **14**.

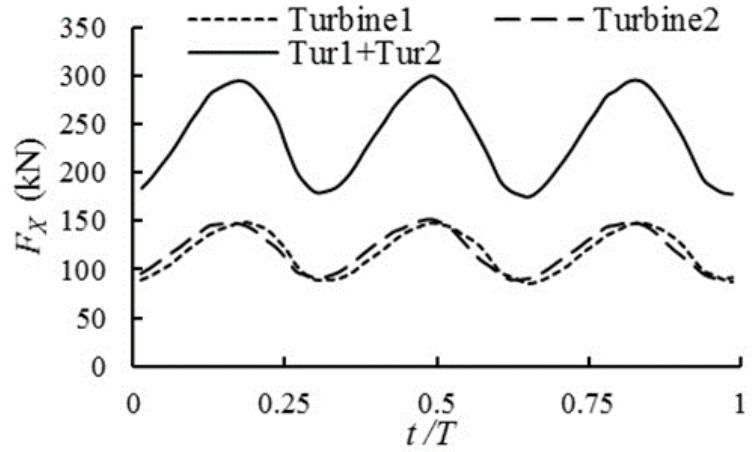

(a) Same rotation

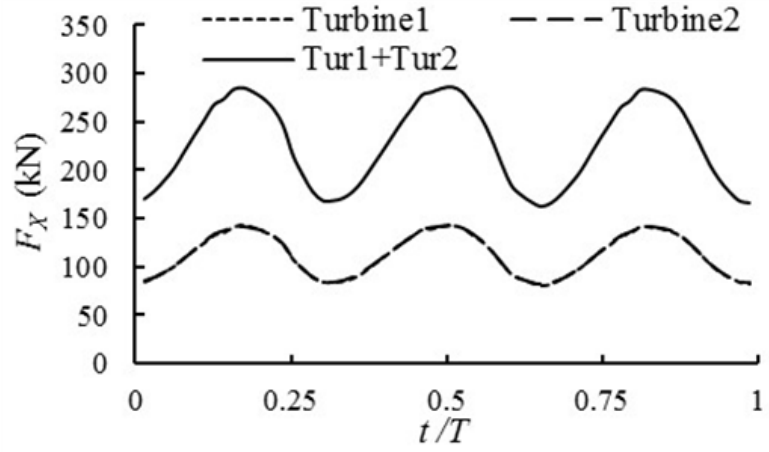

(b) Opposite outward rotation

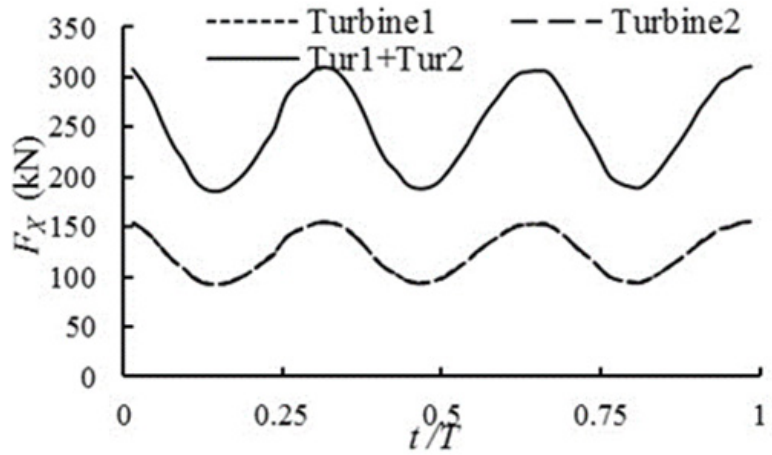

(c) Opposite inward rotation

Figure 13 Thrust of turbines.

The total thrust of turbines with different rotating direction are given in **Figure 13**. For turbines rotating in the same direction, the thrust has 3 periodical fluctuations which are equal to the blade numbers. Forces on turbine1 and turbine2 reach the peak almost simultaneously, with large amplitude. For turbines rotating in opposite inward direction and opposite outward direction,

turbine1 and turbine2 have almost the same thrust values but have the opposite phase angle for inward and outward rotating direction. The average values of total force on 2 turbines are nearly the same, around 230 kN, with the fluctuation amplitude 60 kN, but phase angle of opposite inward rotation is different from the same rotation and opposite outward rotation.

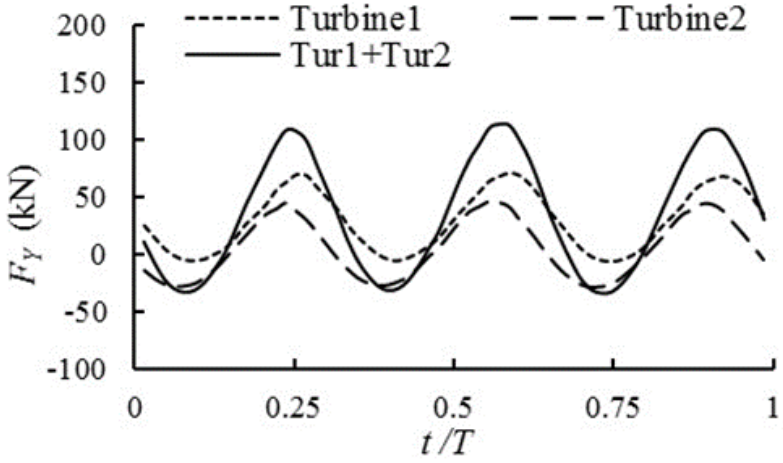

(a) Same rotation

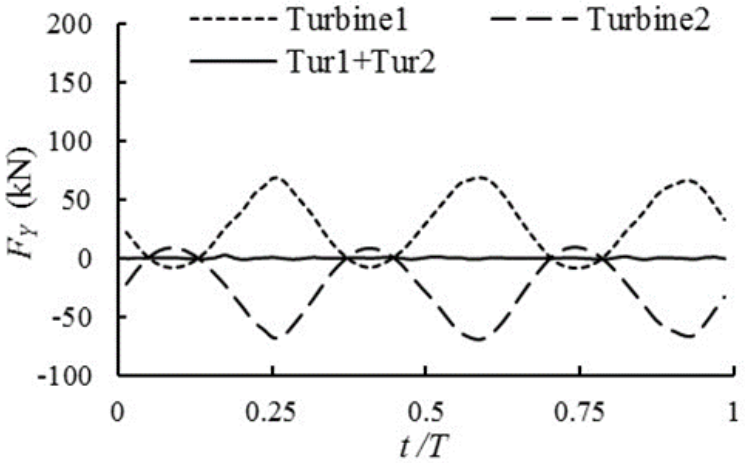

(b) Opposite outward rotation

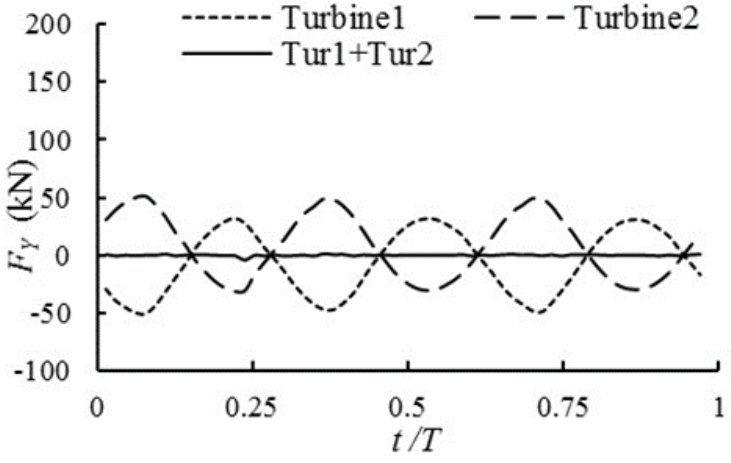

(c) Opposite inward rotation

Figure 14 Lateral force of turbines.

The total lateral force of turbines with different rotating directions are given in **Figure 14**. For turbines rotating in the same direction, the lateral force of turbines has 3 periodical fluctuations which are equal to the blade numbers. Force on turbine1 reaches the maximum peak a little later, and values are a little larger than that of turbine2, which is caused by the flow field overlay. Total lateral force on 2 turbines are larger than that of each turbine in the same rotation direction, which is also larger than that of the other 2 rotation forms. For turbines rotating in opposite outward directions, the lateral force on turbine1 and turbine2 has nearly the same value but an opposite phase angle. Similar results are suitable for opposite inward direction. At the same time, the total lateral force on 2 turbines is almost 0 at any time in one turbine rotating period, which is caused by the symmetry of the flow field. The maximum fluctuation amplitude for turbine1 and turbine2 in opposite outward rotation is a slightly higher than that of opposite inward rotation.

Overall, according to the thrust and lateral force analysis, either opposite inward or outward rotation is a good scheme for parallel twin vertical axis turbines for cancelling the total lateral force and keeping acceptable thrust force on the carrier platform.

4.2.4 Wake characteristics

The wake flow hydrodynamic characteristics of parallel turbines are an influence for the determination of the lateral distance between each row of turbines. When the lateral distance D_y is 1.5D, the wake flow velocity contour and wake flow velocity distribution of 3 kinds of rotation forms are shown in **Figures 15** and **16**. For opposite inward rotation and opposite outward rotation, the velocity contour of parallel turbines wake flow have obvious symmetry; as for the same rotation, the velocity contour of parallel turbine wake flow is asymmetric.

When flow is through parallel turbines, turbine wake flow velocity will greatly reduce; when the distance from turbine to the wake flow is 2D, turbine wake flow velocity is about 30 % of incoming flow velocity; when the distance from turbine to the wake flow is 10D, turbine wake flow velocity is about 50 % of the incoming flow velocity. When the distance from turbine to the wake flow is 2D to 10D and H_d is −0.25D to 0.25D, the wake flow velocity is about 14 % higher than incoming flow velocity; however, the width of velocity growth area is about 0.5D, which is too small for turbine arrangement.

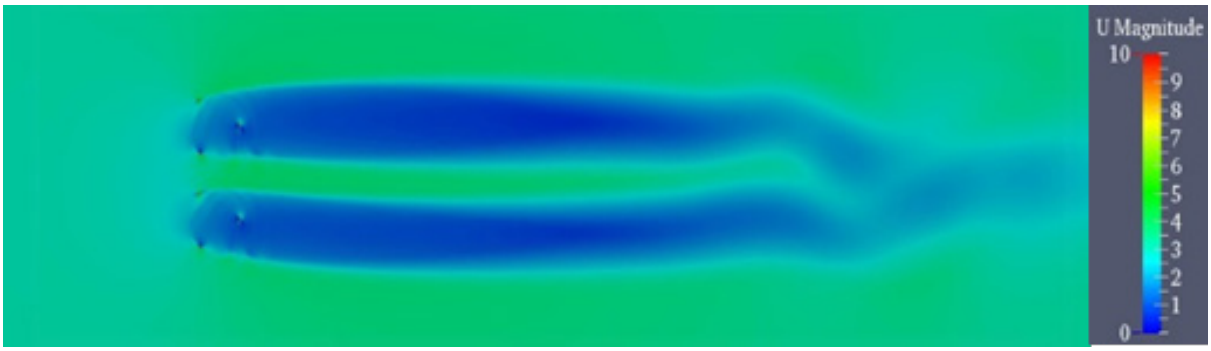

(a) Same rotation

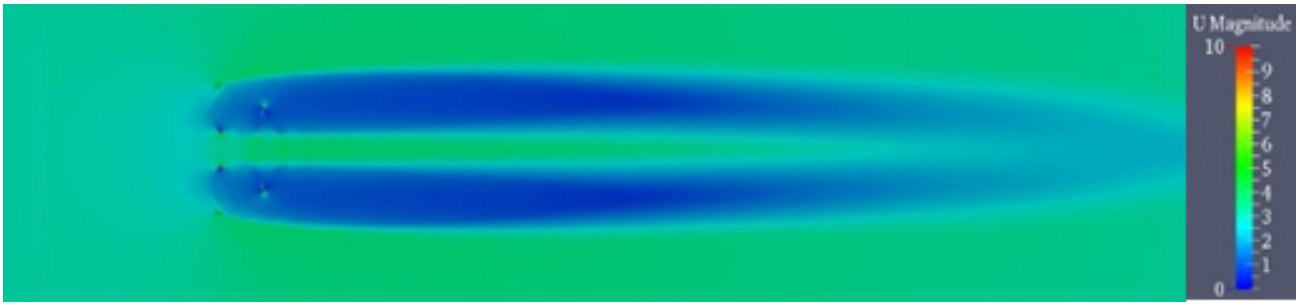

(b) Opposite outward rotation

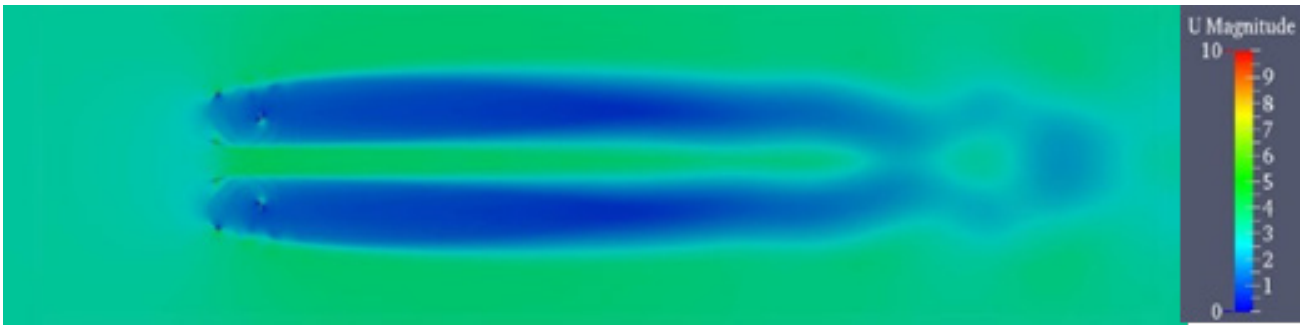

(c) Opposite inward rotation

Figure 15 Velocity contour of flow field (D_y = 1.5D).

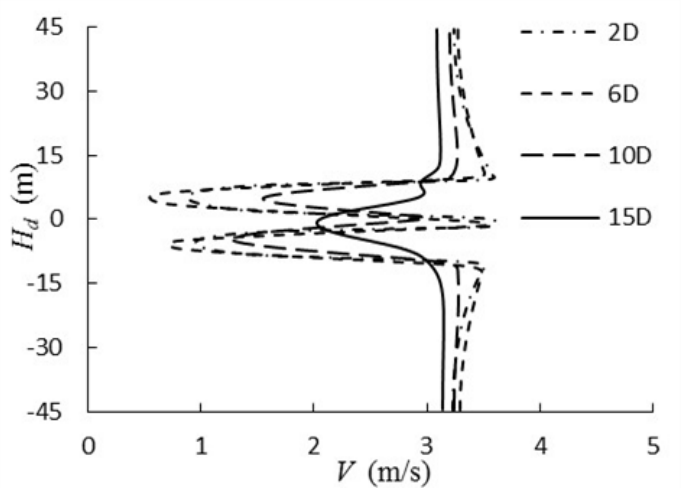

(a) Same rotation

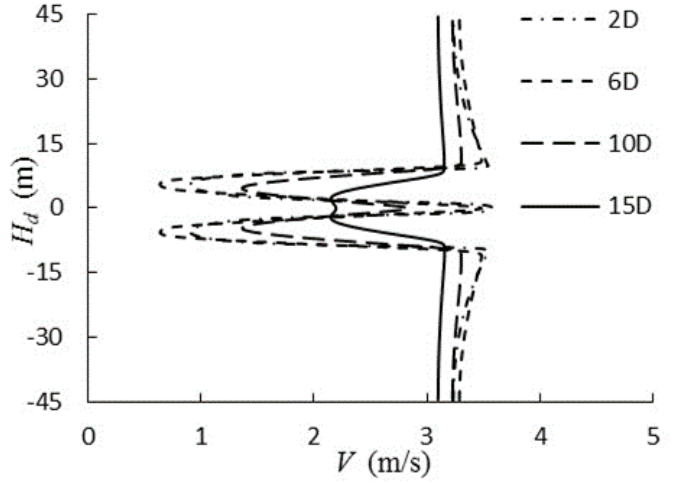

(b) Opposite outward rotation

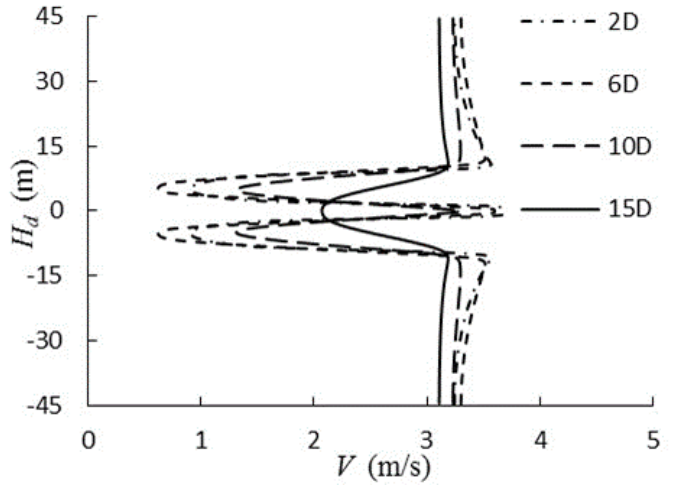

(c) Opposite inward rotation

Figure 16 Velocity distribution of parallel turbine wake flow (D_y = 1.5D).

For opposite inward rotation, the wake flow velocity contour and wake flow velocity distribution are shown in **Figures 17** and **18**, when lateral distance D_y is 1.5D, 2.0D, and 4.0D, respectively. When lateral distance D_y is 1.5D, 2.0D, and 4.0D, the wake flow velocity is approximately 14, 17, and 16 % higher than incoming flow velocity in the velocity growth area, respectively. Moreover, when lateral distance changes from 1.5D to 4.0D, the width of velocity growth area is 0.5D, 1D, and 2.5D, respectively. Therefore, when the lateral distance D_y is 4.0D, it is more beneficial to arrange turbines in the wake flow.

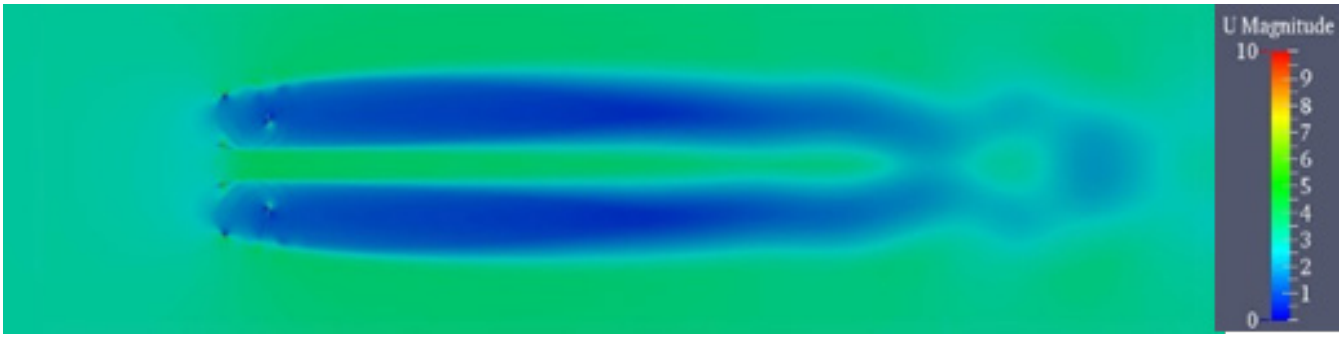

(a) Lateral distance D_y = 1.5D

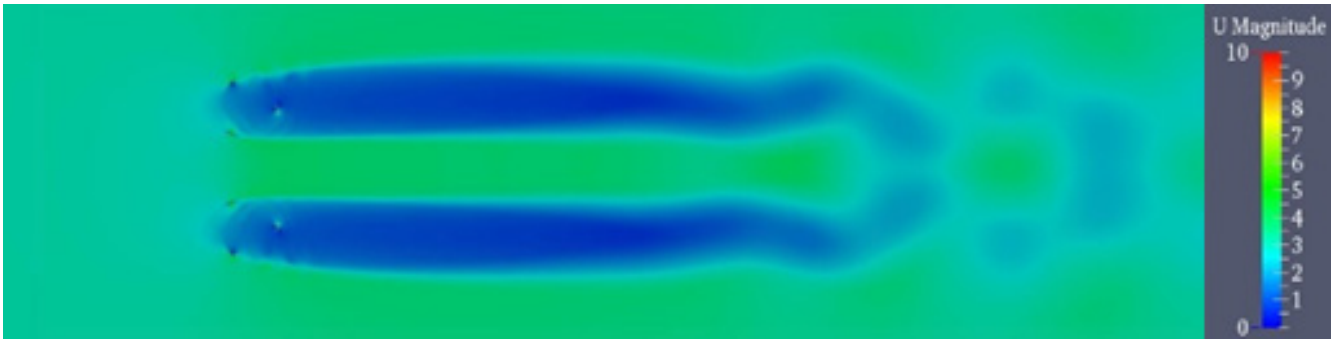

(b) Lateral distance D_y = 2.0D

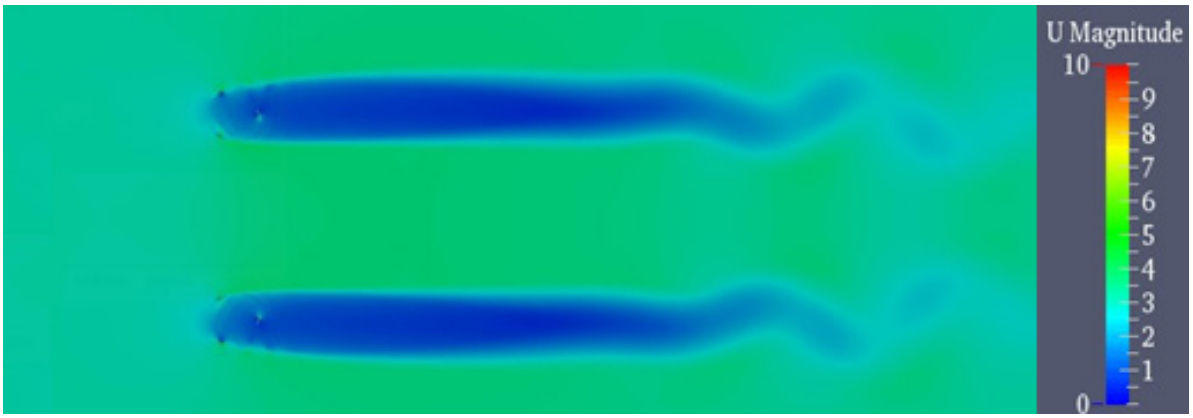

(c) Lateral distance D_y = 4.0D

Figure 17 Velocity contour of flow field (Opposite inward rotation).

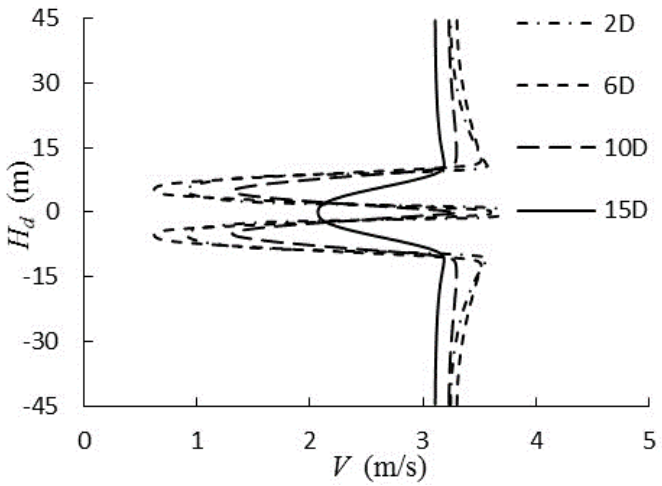

(a) Lateral distance D_y = 1.5D

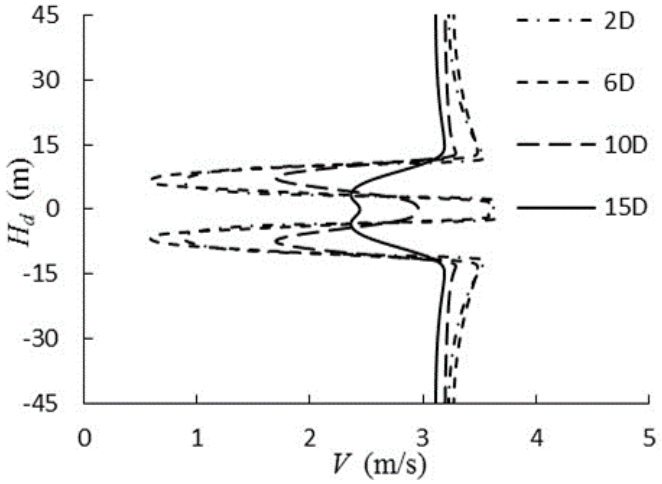

(b) Lateral distance D_y = 2.0D

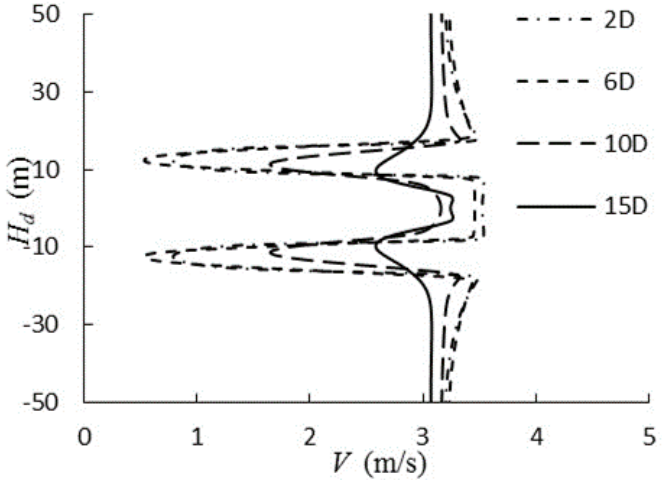

(c) Lateral distance D_y = 4.0D

Figure 18 Velocity distribution of parallel turbine wake flow (Opposite inward rotation).

5. Conclusions

The hydrodynamic performance of parallel twin vertical axis tidal turbines was numerical simulated by the using PimpleDyMFoam solver of open source fluid dynamic software OpenFOAM, including average energy efficiency, blade torque coefficient, thrust, and lateral force on turbines. A single vertical axis turbine by Peter Bachant validated that the 2D numerical model, with reasonable computational domain scale, grid density, k-ω SST turbulence model, PIMPLE algorithm, and proper 3D correction can comparatively forecast the turbine's average energy efficiency accurately. The average energy efficiency of parallel twin turbines is always higher than the single turbine and increases with the increase of the lateral distance between 2 turbines. Additionally, within 3 kinds of rotation forms, average energy efficiency of opposite inward rotation direction is best. When lateral distance approximates to 1.25D and turbines rotate in the opposite inward direction, the average energy efficiency value of the parallel twin turbines is about 25 % higher than that of the single one. For load comparison of turbines with different rotation forms, opposite rotation could cancel the lateral force effect of the total load on the twin turbines and carrier platform. As for wake characteristics of parallel turbines, when lateral distance changes from 1.5D to 4.0D, the width of velocity growth area is 0.5D, 1D, and 2.5D, respectively.

Therefore, for a tidal energy generation platform with parallel twin turbines, opposite outward rotation is the best layout, and the nearest distance between 2 turbines is the best to the extent permitted by equipment installation, operation, and maintenance. Nevertheless, when considering turbine arrangement in the wake flow, it would be better when lateral distance is larger.

References

Bachant, P., & Wosnik, M. (2013). *Performance and near-wake measurements for a vertical axis turbine at moderate reynolds number*. In Proceedings of the ASME 2013 Fluids Engineering Summer Meeting, pp. 1-9. doi:10.1115/FEDSM2013-16575

Dyachuk, E., Goude, A., Lalander, E., & Bernhoff, H. (2012). Influence of incoming flow direction on spacing between vertical axis marine current turbines placed in a row. *American Society of Mechanical Engineers, 7*, 285-292. doi:10.1115/OMAE2012-83347

Gebreslassie, M. G., Tabor, G. R., & Belmont, M. R. (2012). CFD Simulations for sensitivity analysis of different parameters to the wake characteristics of tidal turbine. *Open Journal of Fluid Dynamics, 2*(3), 56-64. doi:10.4236/ojfd.2012.23006

Goude, A., & Agren, O. (2010). *Numerical simulation of a farm of vertical axis marine current turbines*. In Proceedings of the 29th International Conference on Ocean, Offshore and Arctic Engineering. American Society of Mechanical Engineers, pp. 335-344. doi:10.1115/OMAE2010-20160

Guo, F. S. (2013). Performance analysis of vertical-axis tidal current turbines and optimizing turbines array. M. Chinese. Thesis, Dalian University of Technology, Dalian, China.

Jun, D. Shan, Z. D., & Wang X. F. (2010). Research status of tidal current turbine. *Renewable Energy Resources, 28*(4), 130-133.

Kai, W., & Ke, S. (2016). Impact of phase angle on the hydrodynamic performance of a bi-unit vertical axis tidal current energy water turbine. *Journal of Harbin Engineering University, 37*(1), 104-109.

Ke, S., Yan, L., Kai, W., & Liang, Z. (2017). CFD simulation analysis on the wake effect of tandem vertical axis tidal turbines. *Journal of Harbin Institute of Technology, 50*(5), 185-191. doi:10.11918/j.issn.0367-6234.201606097

Lee, J. K., & Hyun, B. S. (2016). Study on performance variation according to the arrangements of adjacent vertical-axis turbines for tidal current energy conversion. *Journal of Korean Marine Environment and Energy Institution, 19*(2), 151-158. doi:10.7846/JKOSMEE.2016.19.2.151

Liang, Z., Li, X. Z., & Jing, G. (2013). Tidal current energy update 2013. *Advances in New and Renewable Energy, 1*(1), 62-63.

Patel, V., Eldho, T. I., & Prabhu, S. V. (2017). Experimental investigations on Darrieus straight blade turbine for tidal current application and parametric optimization for hydro farm arrangement. *International Journal of Marine Energy, 17*, 110-135. doi:10.1016/j.ijome.2017.01.007

Ye, L., & Calisal, S. M. (2010a). Modeling of twin-turbine systems with vertical axis tidal current turbines: Part I-Power output. *Ocean Engineering, 37*(7), 627-637. doi:10.1016/j.oceaneng.2010.01.006

Ye, L., & Calisal, S. M. (2010b). Three-dimensional effects and arm effects on modeling a vertical axis tidal current turbine. *Renewable Energy, 35*(10), 2325-2334. doi:10.1016/j.renene.2010.03.002

Ye, L., & Calisal, S. M. (2011). Modeling of twin-turbine systems with vertical axis tidal current turbine: Part II-torque fluctuation. *Ocean Engineering, 38*(4), 550-558. doi:10.1016/j.oceaneng.2010.11.025

Yong, M., Chao, H., Li, Y., Li, L, Deng, R, & Jiang, D. (2018). Hydrodynamic performance analysis of the vertical axis twin-rotor tidal current turbine. *Water, 10*(11), 1694. doi:10.3390/w10111694